Spectroscopic study of defects and inclusions in bulk poly- and nanocrystalline diamond aggregates

2006 J. Phys.: Condens. Matter 18 L493

(http://iopscience.iop.org/0953-8984/18/40/L01)

INSTITUTE OF PHYSICS PUBLISHING JOURNAL OF PHYSICS: CONDENSED MATTER

J. Phys.: Condens. Matter **18** (2006) L493–L501 doi:10.1088/0953-8984/18/40/L01

LETTER TO THE EDITOR

Spectroscopic study of defects and inclusions in bulk poly- and nanocrystalline diamond aggregates

A A Shiryaev[1], K Iakoubovskii[2], D Grambole[3] and N Dubrovinskaia[4,5]

[1] Institute of Crystallography RAS, Leninsky prospekt 59, 119333, Moscow, Russia
[2] Halfgeleiderfysica, Katholieke Universiteit Leuven, Celestijnenlaan 200 D, 3001 Leuven, Belgium
[3] Forschungszentrum Rossendorf e.V., Institut fur Ionenstrahlphysik und Materialforschung, PF 510119, D-01314 Dresden, Germany
[4] Bayerisches Geoinstitut, Universität Bayreuth, Bayreuth D-95440, Germany
[5] Lehrstuhl für Kristallographie, Physikalisches Institut, Universität Bayreuth, Bayreuth D-95440, Germany

E-mail: shiryaev@ns.crys.ras.ru

Received 5 June 2006, in final form 24 August 2006
Published 22 September 2006
Online at stacks.iop.org/JPhysCM/18/L493

Abstract

Recently, a novel form of nanodiamond exhibiting unusual mechanical properties has been synthesized by high-pressure high-temperature (HPHT) treatment of C_{60} fullerene, amorphous carbon and diamond powder. In this study, we have characterized the dominant defects in this nanodiamond by a combination of optical absorption, luminescence, Raman, electron spin resonance and elastic recoil detection techniques. Unusually high concentrations ($\sim$0.4 at.%) of hydrogen and very low concentrations of nitrogen ($\sim 10^{-5}$ at.%) have been detected in diamond grown from C_{60}. Although most of hydrogen is shown to originate from inclusions of foreign phases, such as water, significant concentrations ($\sim$0.01 at.%) of hydrogen were also detected as a point defect in the nanodiamond grains. Observed structural differences between the samples made from various carbonaceous materials are attributed to different behaviour of the starting compounds during HPHT treatment.

(Some figures in this article are in colour only in the electronic version)

1. Introduction

There is an increasing scientific and applied interest in nanodiamond produced, for example, by chemical vapour deposition (CVD) or detonation synthesis. This interest is due to a number of reasons, including low cost, high production rates, as well as promising prospective applications of nanodiamonds as superabrasives and biocompatible materials (Dubrovinskaia *et al* 2006).

Recently, synthesis of very hard poly- and nanocrystalline diamond aggregates (DAs) with nanosized grains has been reported (Dubrovinskaia *et al* 2005b, 2005a, 2006). In those studies successful synthesis of diamond aggregates was achieved from several carbon phases: fullerene (C_{60}), amorphous carbon (a-C) and microcrystalline diamond powder at very high static pressures (up to 20 GPa) and temperatures (up to 2500 K). The synthesized DAs consist of poly- or nanocrystalline diamond grains, contain several diamond polytypes (ordinary cubic, 2H and 6H hexagonal modifications), and their hardness and bulk modulus are comparable with that of single-crystal diamond. Here we present results of spectroscopic investigation of defects and inclusions in those DA samples.

2. Experimental details

The samples were synthesized from a-C (sample H1927 from Dubrovinskaia *et al* (2005b, 2005a)), diamond powder (S3199) and C_{60} fullerene (Z298) at a static pressure of 25 GPa and temperature of 2300 K using a 6–8 Kawai-type multi-anvil setup at Bayerisches Geoinstitut. The duration of heating was 1 h in all cases. All the samples were thoroughly acid cleaned prior to measurements in order to remove residues of the Pt capsule and other surface contamination.

All characterization was performed at room temperature, except for photoluminescence (PL), which was measured at 80 K. Infra-red (IR) absorption spectra were obtained using a Bruker IFS 120 spectrometer equipped with a nitrogen-purged IR microscope (aperture $\geqslant 50$ μm) with a resolution of 1 cm^{-1}. Every sample was studied at several points in order to assess its homogeneity.

Visible absorption, PL and Raman spectra were recorded with home-built spectrometers. In the so-called 'visible' absorption measurements (spectral range 1.6–5 eV), the sample was mounted on top of a photomultiplier detector in order to reduce light scattering. Luminescence was excited by a N_2 (337 nm or 3.68 eV) laser and detected with a 0.5 m double-grating spectrometer. Raman spectra were recorded under 457.9 nm Ar^+ laser excitation with resolution of 3 cm^{-1}. This excitation line was chosen out of other available Ar^+ lines in order to reduce background PL.

Electron spin resonance (ESR) was measured with a commercial Bruker Q-band spectrometer (microwave frequency $\sim$33 GHz). The signal positions (g values) and concentrations were deduced using a thoroughly calibrated LiF:Li standard, co-mounted with the studied sample. In order to increase accuracy in the signal concentrations, the ESR spectrum was first simulated using a powder-pattern routine. Then the fitting curves were double integrated and compared with the LiF:Li signals (Iakoubovskii and Stesmans 2002a).

The total hydrogen concentration in the samples was measured by elastic recoil detection using a microbeam setup (μERD). For the μERD 12 MeV C^{4+} ions at the nuclear microprobe installed at the 3 MeV tandetron accelerator (Grambole *et al* 2003) were employed. The beam size was $\sim 100 \times 100$ μm^2.

3. Results and analysis

3.1. Absorption and luminescence

Most of the results were obtained from the sample Z298 (Dubrovinskaia *et al* 2005b), prepared from C_{60}. Its Raman and visible absorption spectra are presented in figure 1. While the first-order diamond Raman line at $\sim$1330 cm^{-1} dominates the spectra of diamond aggregates produced from graphite and amorphous carbon, this line has not been detected previously in the material synthesized from C_{60}, when spectra were recorded under 514.5 nm laser excitation

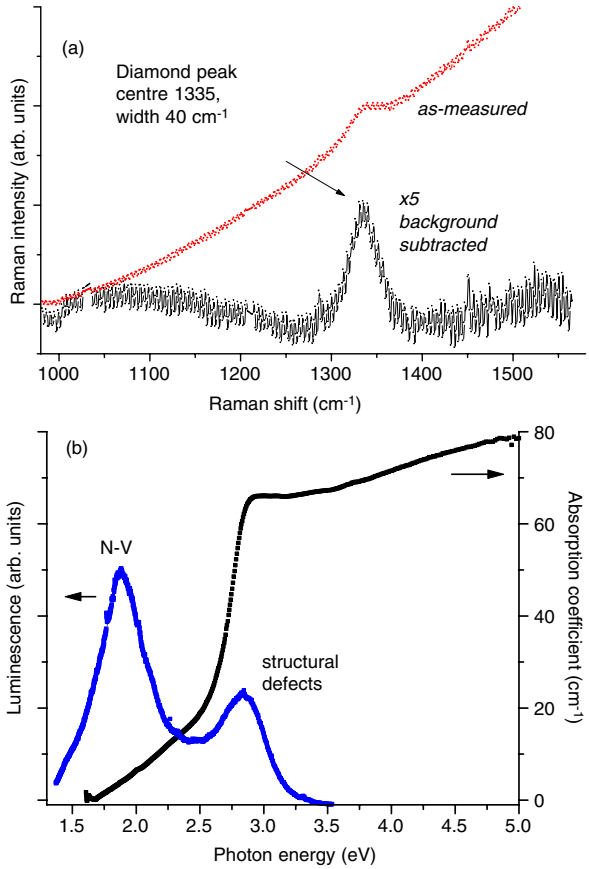

Figure 1. Raman (a), optical absorption and PL spectra of diamond aggregate made from C_{60} (Z298). Raman and PL spectra were recorded under 457.9 and 337.1 nm laser excitation, respectively. Linear background is subtracted from the Raman spectrum.

(Dubrovinskaia *et al* 2005b). In the present study, Raman spectra were recorded using 457.9 nm laser excitation, and a weak diamond peak was observed. It becomes more pronounced after subtracting a linear background (figure 1(a), lower curve). It is clear from the figure that the diamond peak is significantly broadened (FWHM $\sim$ 40 cm^{-1}) as compared to conventional HPHT diamond crystals (typical FWHM $\sim$ 2 cm^{-1}). This broadening could originate from large strain due to small grain size and numerous grain boundaries in the nanodiamond aggregate, as well as due to the high concentration of point defects found in the sample (see below).

The presence of structural point defects and impurities is evidenced by the PL spectrum (left curve in figure 1(b)). The spectrum is dominated by two broad bands centred at $\sim$1.9 and 2.8 eV. Those two bands are universally observed in all synthetic diamonds. They are commonly attributed to the nitrogen–vacancy (N–V) pairs and structural (possibly dislocation-related) defects (Iakoubovskii and Adriaenssens 2000). Note that the PL intensity was relatively weak; considering the very high sensitivity of this technique (up to single defects), we can conclude that the corresponding concentrations are low (ppm level).

Large defect concentrations are also apparent from the visible (right curve in figure 1(b)) absorption spectra. The visible spectrum is similar to that observed in the so-called

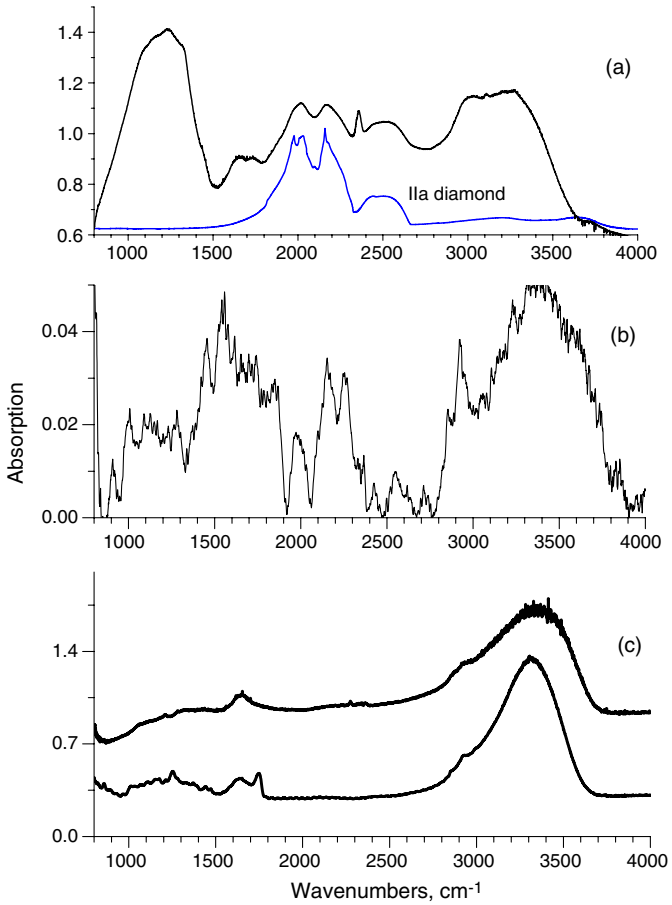

Figure 2. IR absorption spectra of the studied nanodiamonds: (a) sample made from C_{60} (Z298), (b) from diamond powder (S3199), (c) from amorphous carbon (H1927, two different locations). A reference spectrum from pure IIa type HPHT diamond is added to (a) for comparison.

'brown diamonds'—highly strained natural or synthetic diamonds rich in structural defects (e.g. Hounsome *et al* 2006). It is also similar to the spectra of C_{60} treated at high pressures and temperatures (Kozlov *et al* 1997), thus possibly indicating the presence of polymerized C_{60}. Note that the N–V defects detected by PL are not present in absorption, thus again indicating their small concentrations. High resolution transmission electron microscopy (HRTEM) data (Dubrovinskaia *et al* 2005b) has shown that individual diamond grains of the studied diamond aggregate have a perfect diamond structure (note, however, the limited statistics intrinsic to HRTEM), free from extended defects as dislocations, twin boundaries, stacking faults, etc, in agreement with the PL results.

3.2. Infrared spectroscopy

Infrared absorption spectra of the studied samples are shown in figure 2. The IR spectra of diamond compacts contain features due to (a) the diamond lattice, (b) inclusions and (c) bulk defects and surface functional groups in cavities and grain boundaries. The highest quality

spectra were obtained for the DA made from C_{60} (Z298). Compact made from a-C is spatially heterogeneous in its optical properties.

3.2.1. Diamond lattice. Absorption by the diamond lattice (two-phonon process) is present in the spectrum of sample Z298 (C_{60}). In spectra of the DA made from a-C (H1927) or diamond powder (S3199) the lattice bands are hardly detectable. Note, that while the shape of the two-phonon absorption is similar in those two samples, the peaks are much broader in the nanocrystalline DA, thus again indicating large lattice strain.

3.2.2. Inclusions. A strong broad band at 3400 cm^{-1} and a weaker band around 1640 cm^{-1} are present in IR spectra of all samples and are the main features in spectra of the DA made from amorphous carbon. These bands correspond to valence and deformation vibrations of molecular water and O–H groups. Since their intensity is essentially unchanged after acetone and acid treatment, we conclude that the water is present in inclusions sealed between the diamond grains.

A band at 2355 cm^{-1} is due to vibrations of CO_2 molecules. Rotational sub-structure is not resolved in this peak even at high spectral resolution (1 cm^{-1}), indicating that the CO_2 is not gaseous and is probably present in the form of dry ice. The position and relative intensity of this band are sample dependent. In the sample Z298 (made from C_{60}) the band is intense; its shift from the normal position ($\sim$5–7 cm^{-1}) indicates the rather low confining pressure of $\sim$1 GPa (Hanson and Jones 1981). This band is weak in the S3199 and H1927 samples, but the shift is $\sim$12 cm^{-1} (pressure $\sim$2 GPa).

3.2.3. Bulk defects and functional groups. Stretching vibrations of methylene CH_2 hydrocarbon groups were observed in DA made from a-C and from diamond powder. Some hydrocarbon groups are also present in Z298 (C_{60}) sample as a low-energy shoulder on the OH band. A secondary band at 1730–1750 cm^{-1} is observed in all samples. This band could be assigned to the stretching vibrations of C=O bonds in carboxyl and/or carbonyl groups. Absorption in the range 1000–1400 cm^{-1} is from various –C–O–C– groups and/or lattice defects, such as hexagonal polytypes (Klyuev *et al* 1978). Note that structures related to C_{60} polymerization may also contribute to absorption in the Z298 (C_{60}) sample. IR absorption in the range 1000–1400 cm^{-1} is often observed in C_{60} treated at high pressures and temperatures (Kozlov *et al* 1997). The concentration of those defects could be roughly estimated from the absorption intensity as $\sim$0.1 at.%.

3.3. ESR measurements

Figure 3 presents ESR spectra from the studied nanodiamond samples. The spectra were recorded with a low microwave power (1 μW) and modulation amplitude (0.1 mT) in order to avoid signal distortions. No other significant signals were observed in the magnetic field range 30–1500 mT.

The spectrum of the nanodiamond grown from C_{60} is dominated by a strong signal d at $g = 2.0024$ characteristic of a carbon dangling bond. Magnification reveals a number of weak satellites, labelled as a, a', b, b', c and c' on the both sides of the central peak. Signals c, c' and d are commonly observed in CVD diamond (Iakoubovskii and Stesmans 2002b), but to the best of our knowledge they have never been reported for HPHT diamond. The intensity, lineshape and position of the satellite signals were studied here as a function of microwave power and compared with well-characterized CVD samples (Iakoubovskii *et al* 2002). As a result, the signals c, c' and d were unambiguously assigned to the H1 centre (electron spin $S = 1/2$,

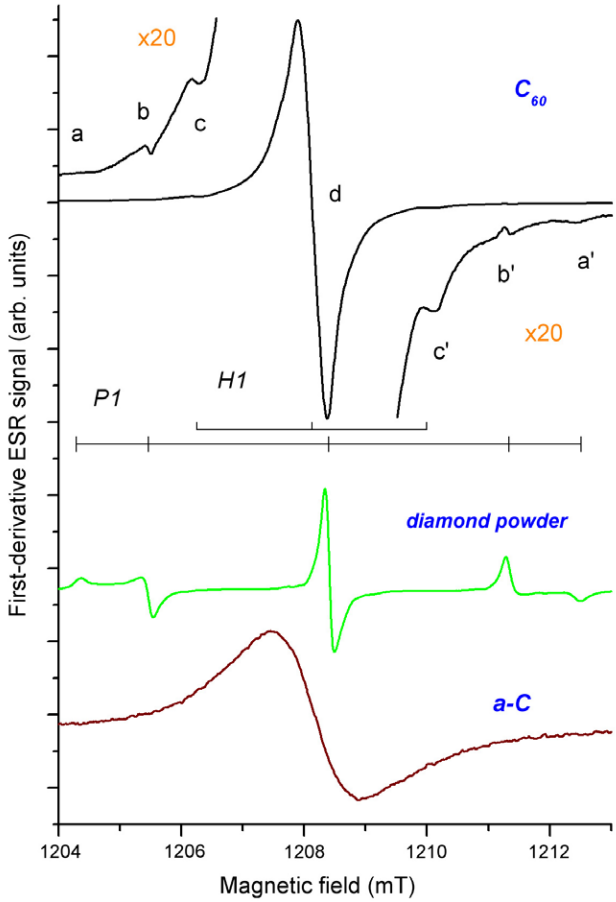

Figure 3. Central part of the Q-band (∼33 GHz) ESR spectra from the nanodiamonds produced from C_{60}, microcrystalline diamond powder and amorphous carbon.

nuclear spin $I = 1/2$ due to one hydrogen atom), and signals a, a', b and b' to the P1 centre ($S = 1/2$, $I = 1$, one nitrogen atom). The central line of the P1 centre could not be identified due to the overlap with the d line. The unusual weakness of the hydrogen-related satellites c and c' in the H1 centre originates from the forbidden nature of the corresponding transitions (Iakoubovskii *et al* 2002). The corresponding concentrations were estimated as 75 parts per million (ppm) for the H1, and 0.1 ppm for the P1 centres.

The discussed H1 and P1 centres are probably the most well known ESR centres in diamond. They are rather abundant and were previously detected at concentrations up to thousands of ppm. The P1 centre is observed in all types of diamond. It is unambiguously assigned to the neutral single substitutional nitrogen. On the contrary, the H1 centre has only been detected in CVD diamond and the polycrystalline diamond variety carbonado (Nadolinny *et al* 2003). It is associated with a neutral bulk defect of trigonal symmetry, involving a C–H bond located next to a carbon dangling bond, possibly a hydrogen–vacancy centre $[H–V]^0$ (Iakoubovskii *et al* 2002).

The ESR spectrum of the sample grown from the diamond powder is dominated by the strong P1 signals. They most likely originate from the initial powder, which is rich in nitrogen.

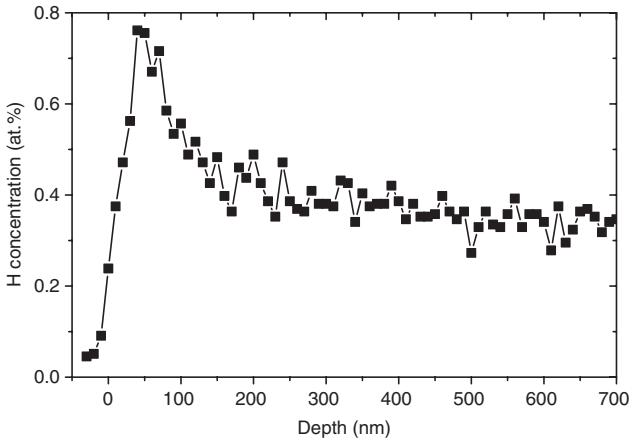

Figure 4. Hydrogen depth profile in the nanodiamond grown from C_{60} measured by μERD.

The spectrum of the a-C grown sample only showed the broad carbon dangling bond signal, which is characteristic of a-C materials. Contrary to the C_{60} case, no hydrogen-related satellites could be detected there because of the large line width.

3.4. Elastic recoil detection

Figure 4 presents a hydrogen depth profile in the sample Z298 (C_{60}) measured by μERD. The total hydrogen concentration is rather high and reaches 0.35 at.%. Significant hydrogen loss has occurred during the measurement. The depletion zone extends to ∼40 nm, which is somewhat deeper than in monocrystalline diamonds analysed under the same conditions. Presumably, a significant fraction of total hydrogen comprises water and other compounds present in microscopic inclusions. In this case, the main contribution to hydrogen loss may be due to decrepitation of those inclusions and concomitant water evaporation.

4. Discussion

One of the important results of the present study is that the grains of nanocrystalline diamond aggregates, synthesized from C_{60} at high static pressures, are almost free from nitrogen-related point defects. On the contrary, monocrystalline HPHT diamond, grown from a-C or graphite, is rich in nitrogen. The origin of this dissimilarity is not yet clear. It may be attributed to different nitrogen species in the growth medium (e.g. N_2, single atoms or N-containing compounds) or to a higher energetic barrier for the incorporation of N into nanograins.

Another topic of this work was to compare nanodiamonds grown from different starting materials (C_{60}, a-C and diamond powder). The present IR absorption and ESR measurements, as well as previous structural characterization (Dubrovinskaia *et al* 2005b), reveal a significant difference in the lattice (e.g. different grain sizes, strain) and defect structure. In particular, FTIR spectra of figure 2 indicate (via the strength of two-phonon absorption) that under nominally the same growth conditions, a higher-quality diamond was obtained from C_{60} than from a-C or (poor quality) diamond powder.

We believe that the principal reason for those differences is the contrasting behaviour of the starting compounds under high pressures and temperatures. It is well known that carbons may be divided into the two broad groups: graphitizing, such as a-C, and non-graphitizing

(e.g. Franklin 1951). The second group represents materials which do not convert to graphite even at 3000 K at ambient pressure. Up to now no complete understanding of the origin of the differences between these two groups exists. Non-graphitizing carbons are often characterized by a low density, high hardness and high porosity on a nanometre scale. One of the models of these materials suggests that they consist of fullerene-like curved carbon sheets (Harris 2005).

Presumably, the size of diamond grains in obtained aggregates depends on the size of the carbon structural units existing immediately prior to the conversion into diamond. During HPHT treatment, amorphous carbon converts into graphite flakes, which, in turn, transform into diamond. On the contrary, during HPHT treatment, C_{60} cages collapse, and different types of bonds between neighbouring molecules are created; amorphization occurs in certain types of treatment (Bashkin *et al* 1994, Iwasa *et al* 1994). The structure of polymerized C_{60} strongly depends on the exact PT conditions of synthesis and on the impurity content of the starting material, but in general products of C_{60} decomposition are closer to non-graphitizing carbons. Since the synthesis experiments were conducted deep in the diamond stability field, the final product consisted almost exclusively of diamond, as shown by x-ray diffraction (Dubrovinskaia *et al* 2005b). Note, however, that XRD is rather insensitive to amorphous materials, and therefore minor concentrations of a-C or amorphous or polymerized C_{60} could remain undetected. Indeed, the ESR spectrum of the a-C grown sample (figure 3) and the FTIR spectrum from the C_{60} grown diamond (figure 2(a)) indicate the presence of unconverted a-C and C_{60}, respectively.

Somewhat surprisingly, the surface chemistry of the studied diamond aggregates is qualitatively similar to that of detonation nanodiamonds (DND). The latter are usually made from organic explosives at pressures between 13 and 30 GPa and temperatures up to 3000 K. The C, O, H, N composition of the precursor, and its interaction with the atmosphere before and during the synthesis, lead to the formation of a broad spectrum of molecules containing C, O, H and N at the DND surfaces (Jiang and Xu 1995). A similar situation is observed for the HPHT nanodiamonds grown from a-C and C_{60}. Indeed, amorphous carbon is rich in C, O and H. The purchased C_{60} powder initially contained mostly carbon; however, due to high surface activity, it quickly adsorbs species containing O, N and H upon ambient exposure. Synthesis of our samples was performed in metal capsules. Diffusion of hydrogen species through the metal capsules is slow and thus the system may be considered as a closed one. Accumulating H-rich gases interfere with complete decomposition of starting carbonaceous compounds to carbon residue. As a result, the surface of the produced nanodiamonds is rich in functional groups related to C, O and H (see FTIR spectra of figure 2).

Pressurized inclusions of water and carbon dioxide are clearly observed in the studied samples. Such inclusions were detected in natural fibrous diamonds many years ago (Chrenko *et al* 1967). The pressure in the inclusions is in the range between 1 and 2 GPa. Knowledge of molar volume and of the equation of state (EOS) of the trapped phase allows the estimation of temperature of inclusion entrapment. At 300 K the molar volume of CO_2 at 1.6 GPa is 28 mol cm^{-3} (Liu 1984). Experimental and theoretical non-parametric EOS for pure CO_2 and a $CO_2 + H_2O$ mixture (Belonoshko and Saxena 1992) indicate that the inclusions reflect lower entrapment pressures than known pressure of the sample synthesis (20 GPa). The simplest explanation is that trapped inclusions have cracked the diamond matrix.

5. Summary and conclusions

The experimental results presented in the previous sections can be summarized as follows. Raman, absorption, ESR and μERD measurements suggest that the studied diamond aggregates contain predominantly diamond, with some H_2O and CO_2 related inclusions present at the

atomic per cent level. The nanodiamond aggregate is highly strained, as indicated by the large width of optical signals, presumably due to high concentrations of structural defects and impurities. Optical and ESR spectroscopies reveal that hydrogen is the dominant impurity in the bulk of diamond grains, while nitrogen, the dominant impurity in HPHT diamond, is present in trace amounts only. This trend has been previously observed (Iakoubovskii *et al* 2000) for nanodiamonds produced by a very different technique, namely explosion synthesis. Note that an opposite behaviour is observed in diamond crystals produced by conventional HPHT synthesis.

The assistance of Dr F Herrmann in ERD measurements is acknowledged. AAS is grateful to the Alexander von Humboldt Foundation and the Foundation of Support of Russian Science for financial support. ND thanks Deutsche Forschungsgemeinschaft for financial support.

References

Bashkin I O, Rashchupkin V I, Kobelev N P, Moravsky A P, Soifer Ya M and Ponyatovsky E G 1994 *JETP Lett.* **59** 258
Belonoshko A B and Saxena S K 1992 *Geochim. Cosmochim. Acta* **56** 3611
Chrenko R M, McDonald R S and Darrow K A 1967 *Nature* **214** 474
Dubrovinskaia N, Dub S and Dubrovinsky L 2006 *Nano Lett.* **6** 824
Dubrovinskaia N, Dubrovinsky L, Crichton W, Langenhorst F and Richter A 2005a *Appl. Phys. Lett.* **87** 83106
Dubrovinskaia N, Dubrovinsky L, Langenhorst F, Jacobsen S and Liebske C 2005b *Diamond Relat. Mater.* **14** 16
Grambole D, Wang T, Herrmann F and Eichhorn F 2003 *Nucl. Instrum. Methods* B **210** 526
Hanson R C and Jones L H 1981 *J. Chem. Phys.* **75** 1102
Harris P J F 2005 *Crit. Rev. Solid State Mater. Sci.* **30** 235
Hounsome L S, Jones R, Martineau P M, Fisher D, Shaw M J, Briddon P R and Öberg S 2006 *Phys. Rev.* B **73** 125203
Franklin R E 1951 *Proc. R. Soc.* A **209** 196
Iakoubovskii K and Adriaenssens G J 2000 *Phys. Rev.* B **61** 10174
Iakoubovskii K, Baidakova M V, Wouters B H, Stesmans A, Adriaenssens G J, Vul' A Ya and Grobet P J 2000 *Diamond Relat. Mater.* **9** 861
Iakoubovskii K and Stesmans A 2002a *Phys. Rev.* B **66** 195207
Iakoubovskii K and Stesmans A 2002b *J. Phys.: Condens. Matter* **14** R467
Iakoubovskii K, Stesmans A, Suzuki K, Sawabe A and Yamada T 2002 *Phys. Rev.* B **73** 113203
Iwasa Y, Arima T, Fleming R M, Siegrist T, Zhou O, Haddon R C, Rothberg L J, Lyons K B, Carter H L Jr, Hebard A F, Tycko R, Dabbagh G, Krajewski J J, Thomas G A and Yagi T 1994 *Science* **264** 1570
Jiang T and Xu K 1995 *Carbon* **33** 1663
Klyuev Yu A, Nepsha V I and Epishina N I 1978 *Dokl. Acad. Sci. SSSR* **240** 1107
Kozlov M E, Tokumoto M and Yakushi K 1997 *Appl. Phys.* A **64** 241
Liu L G 1984 *Earth. Planet. Sci. Lett.* **71** 104
Nadolinny V A, Shatsky V S, Sobolev N V, Twitchen D J, Yureva O P, Vasilevsky I A and Lebedev V N 2003 *Am. Mineral.* **88** 11